Ceramics International 43 (2017) 9408–9415

Contents lists available at ScienceDirect

Ceramics International

journal homepage: www.elsevier.com/locate/ceramint

Enhanced functional response of high temperature stabilized (1-x)PMN-xPT ceramics

Pius Augustine[a,b,*], Martando Rath[a], M.S. Ramachandra Rao[a,**]

[a] Department of Physics, Nano Functional Material Technology Centre and Material Science Research Centre, Indian Institute of Technology Madras, Chennai 600036, India

[b] Department of Physics, Sacred Heart College (Autonomous), Kochi 682013, India

ARTICLE INFO

Keywords:
A. Powders: solid state reaction
B. Grain size
C. Electrical properties
D. Perovskites
E. Capacitors

ABSTRACT

Synthesis of single phase (1-x)Pb($Mg_{1/3}Nb_{2/3}$)O_3-x$PbTiO_3$ ceramics with enhanced electrical response was achieved by excluding excess PbO from the precursor, making them suitable for device applications. This report is an inquiry into the effect of high temperature stabilization used for the realization of single phase PMN-PT ceramics on the electrical properties exhibited by the compositions in the morphotropic phase boundary. Functional response exhibited by the high temperature stabilized ceramics is correlated with the structural fluctuations in the morphotropic phase boundary and the grain pattern observed in the microstructure. Gradual transition from diffuse relaxor ferroelectric system to normal ferroelectric system was also studied. Enhanced ferroelectric response of the composition x=0.35 (P_{sat}=**32.03** μC/cm^2, P_r=**25.11** μC/cm^2, E_C=**6.04** kV/cm, R_{sq}=**1.28**, Absolute area=**3768**, range of electric field=**−37 to +37** kV/cm and recoverable energy density= **59.86** mJ/cm^3), the improved dielectric behavior of the composition x=0.325 ($\varepsilon_{r(max)}$=**15,703**, Tanδ_{max}=**0.02** and γ=**1.79** (at 1 kHz)) and the high piezoelectric coefficient d_{33} (**390** pC/N and **365** pC/N for x=0.325 and x=0.35 respectively), obtained in the study have confirmed the device worthiness of the synthesized ceramic compositions. This study was carried out to establish that, modulated high temperature synthesis will not deteriorate the electrical properties of the lead based system like PMN-PT, rather will assist the completion of perovskite phase formation, and thus enhance the functional response of the ceramic.

1. Introduction

The characteristic phenomenological definition of the relaxor ferroelectric derives from its temperature dependent diffuse phase transition behavior and relaxors exhibit anomaly in the proximity of ferroelectric/paraelectric phase transition with improved electrical response [1,2]. Pure PMN (x=0) is a cubic relaxor material with transition temperature (T_C) ~ 10 °C, whereas PT ($PbTiO_3$) is a normal ferroelectric with tetragonal symmetry and T_C ~490 °C [3]. The addition of lead titanate (PT) causes shift in the B-site group of cations and O^{2-} ions relative to Pb^{2+} ions, which in turn induces non-centrosymmetry in PMN-PT system, resulting in excellent relaxor and ferroelectric properties [4,5]. While pure PMN and (1-x)PMN-xPT with 'x' below 13% exhibit incipient ferroelectric nature with cubic symmetry, the remaining compositions display appreciable ferroelectric response. If the PT content in the solid solution of (1-x)PMN-(x)PT is greater than 40%, it behaves like normal ferroelectric [6]. Among the different compositions, a narrow window with 'x' in the range of 0.31–0.37, called morphotropic phase boundary (MPB), has excellent electrical, optical and electromechanical characteristics making PMN-PT a smart material. Although the response of an ensemble of polar nano regions (PNR) to external stimuli partially explains the behavior of mesoscopic ordered PMN-PT like relaxor material, a unique theory comprehensively illustrating the properties of relaxor material is lacking, despite extensive studies [7,8]. The super-paraelectric model, with the rotation of the resultant electric polarization, or the dipolar glass model with random field, was proposed to describe the behavior of PMN-PT ceramic with a greater degree of accuracy [8]. PMN-PT system is expected to show gradual increase in hysteresis and decrease in strain along the MPB due to the structural change from pseudocubic to tetragonal crystal symmetry [9]. Further, addition of lead titanate (PT) causes substitution of Ti^{4+} ion for complex B-site $(Mg_{1/3}Nb_{2/3})^{4+}$ ion, which reduces the ferroelectric ordering in PMN, and in turn impairs the relaxor character with temperature and dielectric dispersion with

* Corresponding author at: Department of Physics, Nano Functional Material Technology Centre and Material Science Research Centre, Indian Institute of Technology Madras, Chennai 600036, India.
** Corresponding author.
E-mail addresses: piustine@gmail.com (P. Augustine), msrrao@iitm.ac.in (M.S. Ramachandra Rao).

http://dx.doi.org/10.1016/j.ceramint.2017.04.111
Received 23 December 2016; Received in revised form 28 March 2017; Accepted 19 April 2017
Available online 20 April 2017

frequency [2,10,11]. Transition from a short range ordered (nano-domain) relaxor to a long range ordered (micro-domain) ferroelectric with increase in PT and the degeneracy of phases at the morphotropic phase boundary (MPB) are seen as vindication for the smartness of PMN-PT [12,13]. Rotation of polarization vector between adjacent rhombohedral and tetragonal phases through one (or more) temperature dependent intermediate phase(s) of lower symmetry, *i.e.*, monoclinic or orthorhombic or triclinic phase [14,15], and the resulting complexity in domain structure influence the macroscopic property of the ceramic significantly [16]. The axis of polarization, which is along the body diagonal in rhombohedral (*3m*) symmetry, is shifted to face diagonal in orthorhombic (*mm2*) or monoclinic (*Pm*) phases and unit cell edge in tetragonal (*4mm*) symmetry [15]. In the composition range of $32.5 \leq x \leq 35$, the coexistence, of tetragonal (*P4mm*) and monoclinic (*Pm*) phases, is expected due to nucleation barrier to the first order phase transition between high-temperature tetragonal and low-temperature monoclinic phases [17]; and hence expected to exhibit the highest dielectric and piezoelectric response [18]. Also, as the MPB crystal structures are quite mobile and are energetically very close to one another [13,14,19,20] with minor differences in entropy, the structural fluctuations under external stimuli like electric field, stress, temperature *etc.* are favorable for the exhibition of enhanced functional response by PMN-PT system [20].

Inspite of elaborate studies on the PMN-PT system, its utilization in the piezoelectric applications/industry is not extensive owing to two major challenges in the synthesis of PMN-PT, *viz*: i) loss of Pb during synthesis due to vaporization and ii) formation of secondary and paraelectric pyrochlore phase during the synthesis. Formation of covalently bonded parasitic pyrochlore phase must be averted during synthesis to retain the ferroelectric property of the parent phase. Although the widely adopted Columbite B-site precursor method, which uses excess PbO in the precursor, helps in eliminating the pyrochlore phase [21], even a small variation in the local stoichiometry can affect the properties of the prepared ceramics [22]. However, high temperature synthesis will deteriorate the electrical response of PMN-PT system [23]. Device quality 0.65PMN-0.35PT ceramics could be realized using stoichiometric proportion of PbO in the initial precursor by a partial covering method combined with modulated heating regime and a high temperature stabilization [23]. Deciphering the effect of high temperature stabilization on the functional response exhibited by the compositions, along the MPB will ascertain suitability of the method for ceramic synthesis. Piezoelectric, dielectric and ferroelectric properties exhibited by the high temperature stabilized ceramics with compositions x=0.325 and 0.35 are investigated and presented in this report.

2. Material and methods

2.1. Synthesis of PMN-PT ceramic – high temperature stabilization

Solid state reaction route [20] was used for the synthesis of (1-x) PMN-xPT ceramics powders (x=0.3,0.325,0.35 and 0.375). Modulated heating combined with partial covering, which we reported earlier [23], has been used for the realization of stoichiometric and phase pure PMN-PT with compositions spreading over morphotropic phase boundary (MPB). Precursors MgO (Aldrich 99+%) and Nb_2O_5 (Alfa Aesar 99.9+%) were used for the synthesis of single phase columbite-like $MgNb_2O_6$. Stoichiometric proportion of synthesized columbite-like precursor $MgNb_2O_6$ was thoroughly mixed with PbO (Alfa Aesar 99.9+%) and TiO_2 (Titanium (IV) oxide – Aldrich 99.8%). All the PMN-PT compositions analyzed in this report were prepared without using excess PbO in the initial precursor. Thorough grinding of the stoichiometric amount of precursors was done to achieve small particle size which would enhance the phase formation of the perovskite PMN-PT and thereby the functional response exhibited by it. Conventional furnace was used for calcinations and sintering during ceramic preparation. A higher ramp of 10 °C/min in the temperature range of 400 °C to 600 °C and lower ramp of 2 °C/min above 600 °C (modulated heating), were found to be effective in realizing monophasic PMN-PT ceramic. Calcination and stabilization temperatures were fixed at 850 °C for 6 h and 1050 °C for 4 h respectively. After the phase confirmation of the synthesized ceramics using X-ray diffraction and Raman spectroscopy [XRD – PANalytical X'Pert Pro – Cu Kα radiation having wavelength=1.5418 Å and Raman spectroscopy - Olympus BX41 HoribaJobin- Yvon LabRAM HR800 UV–vis Raman set up Ar ion laser (488 nm) as excitation source], powder samples were compacted for sintering. Samples were mixed thoroughly with 5% PVA (two drops for 5 g sample) and cold compaction was done in tungsten carbide die set (top punch- tungsten carbide brazed with steel) giving uniaxial pressure of 350 MPa for 5 min; and an optimized sintering temperature of 1150 °C for 4 h was administered to the samples during densification. Synthesis chemistry and the special crucible assembly used were thoroughly discussed elsewhere [23]. Ferroelectricity being a phonon originated /generated phenomenon; a temperature varying Raman spectroscopy of the compacted pellets was carried out to characterize the phonon modes, if any. Raman spectrometer was calibrated with the standard silicon sample (Si) at band position, 520.5 cm^{-1} and room temperature Raman spectra were recorded at various points on the surface of the pellets to ensure homogeneity of the sample, before starting the temperature varying measurements. A flag sketch showing the heating conditions and phase formations is depicted in Fig. 1.

2.2. Characterization and functional property measurements

Apparent densities of the as sintered pellets were determined using Archimedes' water displacement method. After polishing both sides of the sintered pellets using fine silicon carbide abrasive sheet (P1200) and measurement of dimensions, silver paint was applied on either side and fired to form electrodes for the electrical measurements. Firing of the silvered pellets were carried out in a box furnace under ambient atmosphere at 625 °C for 30 min, which ensured the depoling of the material and relieving of the internal stress, if any, induced during the preparation of the sample. Also, firing ensures that pure silver electrodes are left on the sample, as the polymer part of the silver paint will be burnt out. Electrical properties of the two PMN-PT compositions (x=0.325 and x=0.35) were then carried out and correlated with the structure and microstructure exhibited by the samples. Dielectric studies were carried out [Alpha High Resolution Dielectric/Impedance Analyzer (Novocontrol)] over a wide range of frequencies 1 Hz to 100 kHz (data for only 100 Hz to 100 kHz are shown) and ferroelectric responses were determined at a fixed frequency (12 Hz). Ferroelectric measurements were done using the ferroelectric loop tracer [Radiant PE loop tracer (Radiant Technologies, USA)] after calibration. Voltage applied across the specimen was gradually increased in steps of 20 V to 50 V. Measurements were taken for a varied frequency ranges, after a rise of every 400 V to 500 V, to stabilize the dipolar response to the applied electric field. The squareness in the P-E

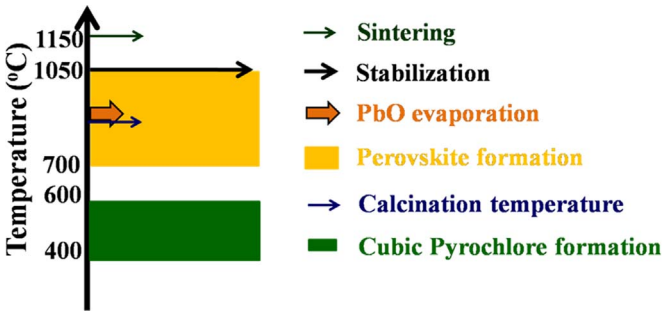

Fig. 1. Flag diagram showing the heating conditions and phase formation.

loops traced for the samples were calculated using the empirical expression $R_{sq}=P_r/P_{max}+P_{1.1Ec}/P_r$, where P_{max} is the maximum polarization obtained at a finite field strength below dielectric breakdown, P_r is the remnant polarization and $P_{1.1Ec}$ is the polarization at an electric field equal to 1.1 times the coercive electric field [10]. Recoverable energy densities of the compositions are obtained by subtracting the calculated area from the total area, and it represents the available energy per unit volume of dielectric on discharge. Dielectric measurements were carried out during cooling from 300 °C to the room temperature thus avoiding error due to degassing. The temperature decrease during measurements was fixed at steps of 5 °C in the range from 190 °C to 140 °C to ensure better response around T_C, whereas the remaining steps were set at 10 °C variations. Analyses of the variation in the real part of dielectric permittivity (ε′) and dissipation factor (tanδ) with temperature and frequency, as the samples were cooled through the transition at a rate of 3 °C/min, were carried out. Analyses of relaxor exponents were also done to establish the relaxor behavior of the MPB compositions. Before taking the piezoelectric measurements, samples were poled in the ambient atmosphere (no silicone oil or grease was used) in a conventional furnace, at 160 °C (near the dielectric maximum temperature T_m). Poling was carried out by applying a gradually increasing voltage, in steps of 25 V for 30 s each, until the electric field becomes nearly equal to the coercive electric field (~6 kV/cm). The sample under test was then retained at this temperature and field for 20 min and then allowed to cool while holding the electric field. Piezoelectric responses (d_{33}) of the poled targets were then measured using a 'quasi-static' or 'Berlincourt' type Piezo d_{33} meter (Sinocera-YE2730A) at 110 Hz. To correlate the functional response with microstructure, SEM images were taken on the fractured pellets using Quanta 400FEG scanning electron microscope.

3. Results and discussion

3.1. Synthesis and stabilization

A crucial pre-requisite in solid state reaction is fine and well mixed precursor, achieved by thorough grinding, to facilitate the proximity of the chemicals during thermal treatments and chemical homogeneity of B-site cations. Sintering kinetics greatly depends on the particle size; reduced particle size reduces the path length for atomic diffusion which accelerates the densification process and enables attainment of chemical equilibrium at a lower temperature. Rapid heating up to 600 °C during sintering prevents the formation of cubic and non-ferroelectric pyrochlore phase, which slows down the possible conversion of PbO to Pb_3O_4 ($PbO_{1.1/3}$) [24], whereas the slow heating above 600 °C ensured the conversion of Pb_3O_4 back to PbO (if at all formed) and formation PMN-PT perovskite phase. After calcination at 850 °C for 6 h, gradual heating of samples, at the rate of 2 °C/min up to 1050 °C, ensured the completion of perovskite formation. If the mixed precursor is directly heated to 1050 °C, enhanced Pb evaporation and resulting PbO deficit would lead to the formation of secondary pyrochlore phase in the composition. Perovskite PMN-PT formed was retained at 1050 °C for 4 h, and is referred to as *'stabilization heating'*. Since the melting temperature of perovskite PMN-PT is above 1280 °C, stabilization heating would not affect the perovskite PMN-PT phase and would rather maximize the formation of single phase perovskite PMN-PT ceramics.

3.2. X-ray diffraction and Raman spectroscopy

Fig. 2 shows the X-ray diffractogram of the synthesized (1-x)PMN-xPT samples (x=0.30, 0.325, 0.35 and 0.375) in the morphotropic phase boundary. Samples exhibit pure perovskite phase without trace of any secondary phase. Strongest diffraction peak of pyrochlore phase at 2θ≈29° was not detected in any of the compositions (samples)

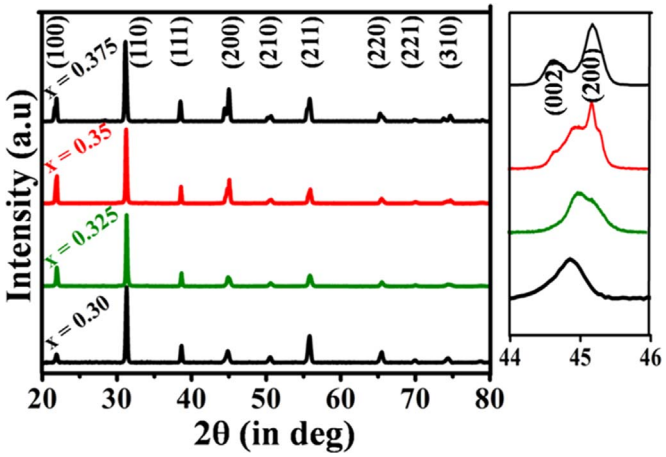

Fig. 2. X-ray diffractograms of (1-x) PMN-x PT ceramic pellets (x=0.30, 0.325, 0.35 and 0.375) prepared without excess PbO in the initial precursor. Magnified region (2θ =44°–46°), which is shown at the right side indicates the coexistence of phases which is expected in the case of PMN-PT compositions in the MPB. (No pyrochlore phase is observed).

studied. Analysis of the diffractogram at 2θ=44°–46° vindicates the presence of a mixed crystal symmetry, particularly in the compositions x=0.325 and x=0.35, which is expected in the case of PMN-PT compositions in the MPB region. Rietveld analyses of the selected compositions (x=0.325 and 0.35) were carried out using Fullprof suite software (not shown). While the composition x=0.325 exhibited best fit with monoclinic (*Pm*) symmetry, x=0.35 exhibited best fit when mixed phases - monoclinic (*Pm*) and tetragonal (*P4mm*) - were tried. Thompson-cox-Hastings-pseudo-Voigt profile shape function was used for fitting the XRD pattern of both the compositions.

Raman spectroscopy analyses of the synthesized ceramics (x=0.325 and x=0.35), at room temperature (Figs. 3(a) and (b)) and in the temperature range where dielectric study exhibits considerable variations with temperature (Figs. 4(a) and (b)), were done to confirm the phase purity. The peaks observed in Raman spectrum corresponding to various modes, are similar to earlier reports and were attributed to different vibrations *viz.*, 270 cm^{-1} to O-B-O, 450 cm^{-1} to Mg-O, 580 cm^{-1} to B-O-B and 790 cm^{-1} to B-O-B′ (B and B′ stand for Nb or Ti). The sharp and intense peak at around 270 cm^{-1} corresponds to the perovskite peak and validates enhanced perovskite formation due to stabilization heating applied during ceramic synthesis. The peak at 740 cm^{-1} is of special interest in this study as it indicates the coexistence of mixed phase, which arises due to the change in local symmetry associated with MPB region. Also, the broad peaks with low resolution observed at room temperature and in the temperature varying Raman spectra, confirm the relaxor-ferroelectric behavior of the material [25–27]. No significant difference in modes of vibration was observed between the Raman spectra (Fig. 3 and 4) at room temperature and in temperature variation studies of both compositions (x=0.325 and x=0.35). Hence, the ferroelectric and dielectric properties exhibited by the synthesized ceramics in response to applied electric field and temperature can be attributed to the structural fluctuations from pseudocubic to tetragonal symmetry through intermediate low symmetry monoclinic and/or orthorhombic structures and the associated free energy variations [28], rather than the variation in modes of vibration.

3.3. Electrical properties in the morphotropic phase boundary

3.3.1. Analysis of ferroelectric response

Polarization (P) *vs* Electric field (E) study is the single most powerful characterization tool and the fingerprint of any ferroelectric system. Fig. 5 shows symmetrical hysteresis loop traced by the samples prepared in the present study. Since, the coercive field (E_C) is a

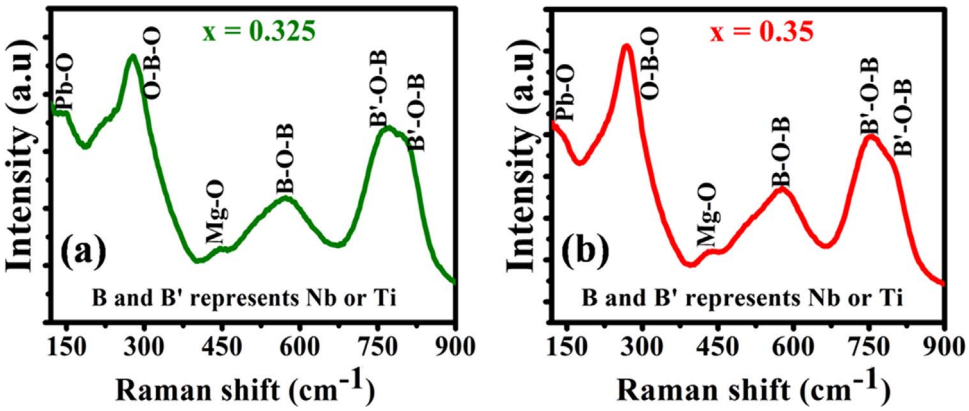

Fig. 3. Raman spectra of a) 0.675PMN-0.325PT and b)0.65 PMN-0.35 PT pellets at room temperature, (pellets were made without using excess PbO in the initial precursors.) (Various modes responsible for the peaks are shown. Ar laser having wavelength 488 nm was used for excitation.).

measure of the energy barrier to the B-site cations; increase in the value of coercivity E_C of the PMN-PT solid solution compared to pure relaxor is an indication that B-site cations encounter higher jump barrier or need large external field to switch the occupying sites [29]. Lack of square hysteresis as evident from R_{sq} values indicates the absence of long range cooperation among dipoles required for normal ferroelectrics. Higher remnant polarization which is seen in phase-pure samples may be due to the reversion of 180° and non 180° domains under high electric field applied [19].

Higher values of saturation and remnant polarizations, large absolute area, wide range of electric field which the sample could withstand and the large grain microstructure with clean grain boundaries exhibited by the composition x=0.35 (Table 1), confirm the suitability of the composition for ferroelectric applications. Larger value of saturation polarization (P_{sat}=32.03 μC/cm^2) exhibited by the composition x=0.35, may be attributed to the deformation of the lattice [23]. Value of the polarization (P=29.68 μC/cm^2) exhibited by the composition x=0.35 at E =15.92 kV/cm (maximum electric field obtained in the composition x=0.325), is also shown for better comparison (Fig. 5). Higher value of polarization obtained in the composition x=0.35 (P=29.68 μC/cm^2) compared to that in the composition x=0.325 (P=23.93 μC/cm^2), at the same maximum electric field could be attributed to the degeneracy of phases in the composition x=0.35, with an increased percentage of the tetragonal symmetry due to the increase in $PbTiO_3$. Also, an increase in tetragonal symmetry in the composition will facilitate a long range ordered microdomain in the composition x=0.35 [12,13],which is favorable for improved ferroelectric response. Available literature on the quantitative study on the energy storage and energy harvesting ability of the ceramics is sparse, mainly due to the reduced dielectric strength of the material prepared through conventional techniques. Fig. 6 shows the increased recoverable energy density of the composition x=0.35, which attest the enhanced energy harvesting ability of the same compared to x=0.325 composition [28]. Recoverable energy density calculated for the composition x=0.35, for the value of maximum electric field (E=15.92 kV/cm) exhibited by the composition (x=0.325) is also given for better comparison (Fig. 6c). The response could be attributed to the mixed crystal symmetry seen in the composition x=0.35. Change of shape of PE hysteresis loop from slim to square with increase in PT is evident from the absolute area calculated (2715 for x=0.325 and 3768 for x=0.35); and it may be attributed to the increase in tetragonality of the composition.

3.3.2. Dielectric response

The analyses of the dielectric response in the frequency range (100 Hz to 100 kHz) of the two compositions (x=0.325 and 0.35) are shown in Figs. 7–9 and Table 2. Enhanced dielectric constant exhibited by the samples may be attributed to the increase in the grain size (Fig. 10) [30], which enables easy switching of domains [18]; and the higher density [31] exhibited by the ceramic pellets (Table 3). The reduction in the non polar grain boundary, with increase in grain size, favors dielectric response exhibited by the ceramics.

Since, a pronounced shift in T_m towards higher temperature with frequency was not evident in the dielectric response of the selected compositions (x=0.325 and x=0.35), dielectric analyses was done using Lorentz type relaxation behavior [13]. With the increase in tetragonality, a decrease in dielectric constant and an increase in dielectric loss were observed as expected due to restricted mobility of the domains [19]. Significant reduction in the dielectric dispersion observed in our study, corroborates the earlier reports, for the compositions in the MPB

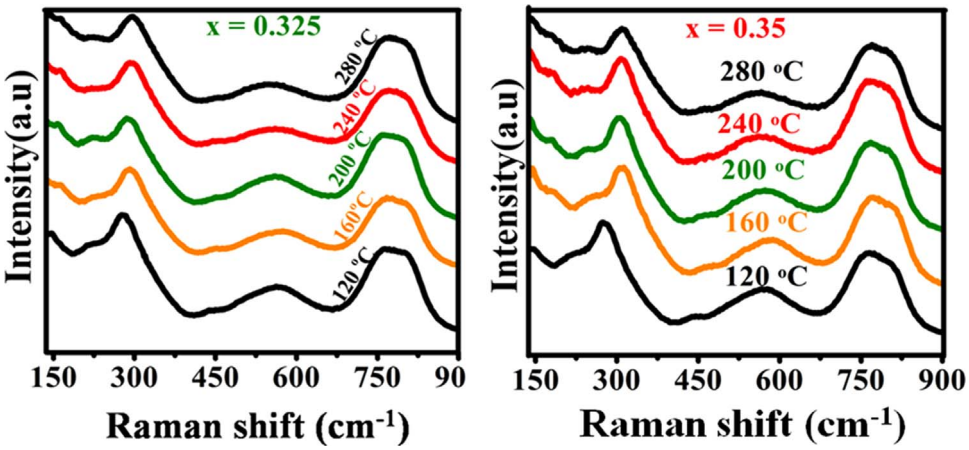

Fig. 4. Raman spectra of a) 0.675 PMN-0.325 PT and b) 0.65 PMN-0.35 PT pellets at various temperatures in the range where it show abrupt change in dielectric response.

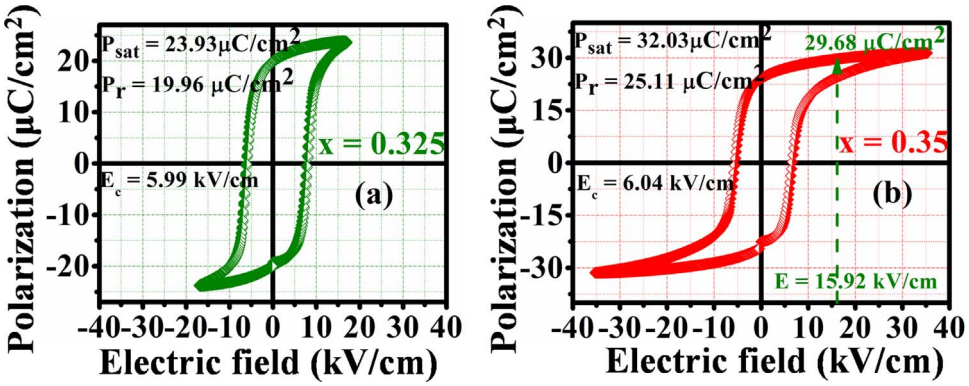

Fig. 5. Ferroelectric response (Polarization *vs* Electric field) graphs of a) 0.675 PMN-0.325 PT and b) 0.65 PMN-0.35 PT. (Value of the polarization (P=29.68 μC/cm^2) exhibited by the composition x=0.35 at E=15.92 kV/cm, is also shown for better comparison).

region [11,13]. Although both samples exhibited dielectric dispersion, composition x=0.325 exhibited better dielectric behavior compared to x=0.35, which can be attributed to the higher proportion of rhombohedral symmetry in x=0.325. Variation of real part of dielectric permittivity (ε′) and loss tangent (tanδ) with temperature (T) and frequency (*f*) exhibited by the samples were analyzed (Figs. 6 and 7). The characteristics of the temperature dependent dielectric permittivity of a relaxor ferroelectric material can be described using modified Curie-Weiss law, which is given below.

$$(1/\varepsilon)-(1/\varepsilon_m) = [(T-T_m)^\gamma]/C- \quad (1)$$

where ε_m is the maximum value of dielectric permittivity at the transition temperature (T_m), C is the Curie-like constant and γ is the value of relaxor factor or Curie-Weiss exponent ($1\le\gamma\le2$). The degree of dielectric relaxation can be determined from the slope of $\log_{10}[(\varepsilon_m/\varepsilon)-1]$ *vs* $\log_{10}(T-T_m)$ plot (Fig. 8). If γ=1, Eq. (1) describes Curie-Weiss behavior of normal ferroelectrics, while it corresponds to perfect relaxor ferroelectrics with a clean diffuse phase-transition behavior if γ=2 [13,32]. A comparison of dielectric response of the two samples is shown in Table 2. The relaxor exponent value ($\gamma > 1.7$) confirms a diffuse type first order ferroelectric-paraelectric phase transition [33]. The maximum temperature (T_m), which corresponds to the ferroelectric-paraelectric phase transition, is found to be approximately 177 °C and 165 °C respectively for the compositions x =0.35 and x=0.325.

At the tested frequencies, the full width at half height of the dielectric peaks of the samples, was found to be around 50 °C, as expected for bulk PMN-PT ceramics at the morphotropic phase boundary, due to the co-existence of multiple phases [34]. No prominent response or dielectric peak was observed at temperatures below 100 °C, in either of the compositions. Dispersion of permittivity above T_m, observed in this study against PMN-PT single crystal data, may be attributed to the presence of low permittivity passive dielectric layer at the electrode ceramic interface [7]. The observed merging of dielectric absorption graphs at considerably lower and higher temperatures than T_m indicates the relaxor properties of the samples. Merging in the absorption graphs was found to be more prominent in x=0.325, and the same may be ascribed to the increased relaxor characteristics due to the shift in the crystal symmetry towards rhombohedral side of MPB. However, no appreciable difference in the behavior of tanδ with temperature was observed in either of the compositions, as the crystal symmetry of the sample changes from rhombohedral to tetragonal phase along the MPB region. Identical grain size distribution in both compositions possibly resulted in similar tanδ as well as equality in coercivity (E_C). Heat transfer occurs in quantum jumps, and the associated loss of electric energy becomes crucial at high frequencies. Therefore, the low energy loss at high frequencies observed in our study (Fig. 8), also establishes the outstanding quality of the synthesized ceramics.

3.3.3. *Effect of poling and piezoelectric response*

Prior to testing for piezoelectric response, the samples were subjected to poling and no arcing was observed during the procedure. The poled samples were kept in polythene case under ambient conditions free from any electrical or thermal interference. Charge per unit force in the direction of polarization [piezoelectric coefficient (d_{33})] is an important material property, which decides the suitability of the ceramic for actuator applications. High piezoelectric response (d_{33}) was observed in the samples even at three months after poling (Table 3). Enhanced piezoelectric properties may be attributed to the change in crystal symmetry of the material, which takes place under the application of an electric field above the characteristic critical field of the material. New symmetry will be retained as long as the ceramic is not subjected to extreme temperature conditions (annealing above critical temperature) or mechanical treatments (powdering/ crushing) [15]. Enhanced piezoelectric response exhibited by the x=0.325 composition may be attributed to the presence of mixed phases of rhombohedral and monoclinic symmetry in the sample [9]. Also, piezoelectric coefficient (d_{33}) being an anisotropic quantity, the variations in the response may be ascribed to the difference in the percentage of the unit cell orientations inside the specimen. Low E_c was found to be favorable for poling and in combination with higher P_r ensured increased piezo-response after poling. Enhanced piezoelectric response exhibited by the specimen after field cooling could be attributed to the easy mobility of the crystal structure at the MPB [19]. Promising d_{33} value exhibited by the ceramic establishes the

Table 1
Comparison of ferroelectric data of 0.675PMN-0.325PT and 0.65PMN-0.35PT samples. (Polarization and energy density for composition x=0.35, at/for E=15.92 kV/cm is also given for comparison of the data with composition x=0.325).

	P_{sat} μC/cm^2	P_r μC/cm^2	E_c kV/cm	$P_{1.1Ec}$ μC/cm^2	R_{sq}	Absolute area	Range of E kV/cm	Recoverable energy density (mJ/cm^3)
PMN-PT x=0.325	23.93	19.96	5.99	9.25	1.27	2715	−16 to +16	19.877
PMN-PT x=0.35	32.03 (29.68 at E=15.92 kV/cm)	25.11	6.04	12.54	1.28	3768	−37 to +37	59.86 (31.41 for E_{max}=15.92 kV/cm)

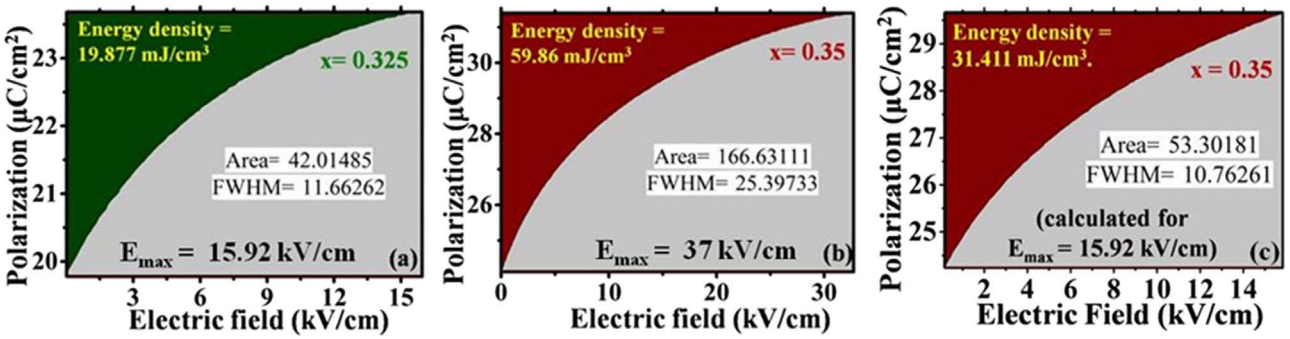

Fig. 6. Energy density calculation using Origin software. Recoverable energy densities from the compositions (a) x=0.325 (19.87 mJ/cm^3), (b) x=0.35 (59.86 mJ/cm^3) and (c) x=0.35 (31.411 mJ/cm^3, at E_{max}=15.92 kV/cm. Energy density is determined by subtracting the shaded area calculated from the software from the total area. (x=0.35 is showing higher recoverable energy density).

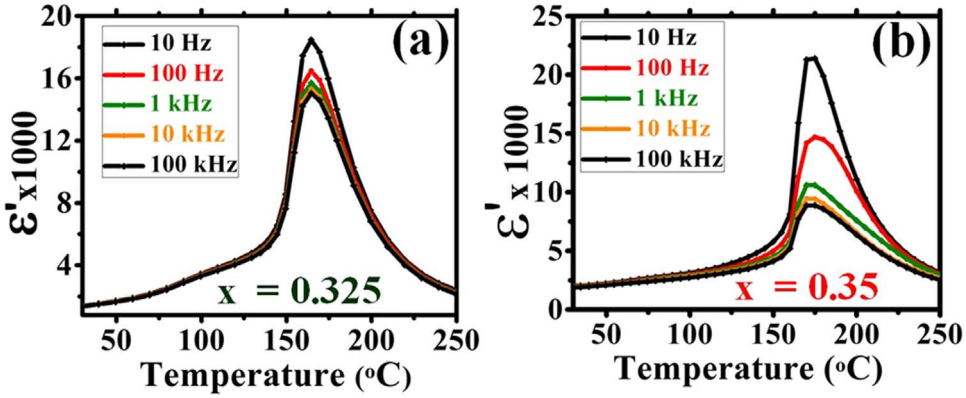

Fig. 7. shows temperature variation of real part of dielectric permittivity (ε') at various frequencies. a) 0.675PMN-0.325PT and b) 0.65PMN-0.35PT. Shift in Tc (~165 °C for 0.675 PMN-0.325 PT, ~177 °C for 0.65 PMN-0.35 PT) seen may be due to the transit of the composition from diffuse relaxor to normal ferroelectric along the MPB.

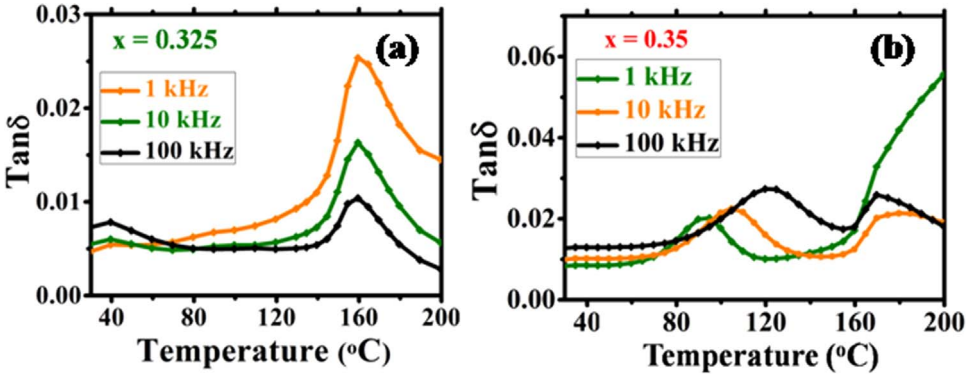

Fig. 8. Temperature dependence of loss tangent exhibited by a) 0.675 PMN-0.325 PT and b) 0.65 PMN-0.35 PT, at various frequencies. (Tanδ values are shown only for higher frequencies). Loss tangent values at high frequency are found to be very low, which attest the quality of the ceramic samples prepared. Increase in loss tangent observed for 0.65 PMN-0.35 PT compared to 0.675 PMN-0.325 PT may be due to the decrease in the mobility of domains in the tetragonal structure.

absence of pyrochlore phase and the effectiveness of the high temperature stabilization synthesis adopted for its preparation. Ferroelectric and piezoelectric responses exhibited by the compositions were found to be comparable or superior to the values reported earlier on the similar compositions (Table 4).

3.4. Density and microstructure analysis

Densities of the samples were determined by hydrostatic weighing in de-ionised water (Archimedes' method) under ambient atmosphere (Table 3). Higher density (95% or above) obtained for the samples can be attributed to the absence of pyrochlore phase in the ceramics and fine particle size achieved by thorough grinding [35]. High density obtained in our study is an indication of the absence of pores in the sample, and explains the enhanced electrical response exhibited by the ceramics. Water or other liquids occupying the pores, if present, would increase the dielectric loss, which in turn would make the ceramic hard to pole, and result in inferior piezoelectric behavior. Though an increase in density of the ceramic is expected with PT addition to PMN, nearly equal density of the compositions observed in our study must be due to the narrow range, x=0.325 to 0.35 of PMN-PT, selected. Although a higher PT content warrants high sintering temperature, higher density obtained at comparatively lower sintering temperature in our synthesis could be attributed to the thorough grinding given to the sample before and after calcinations. Low sintering temperature and high dielectric constant of the synthesized material indicates the suitability of the ceramic for multilayer capacitor (MLC) applications.

In addition to the processing and poling procedures, the functional properties of the PMN-PT ceramic samples have a strong dependence on the grain size of the material system. Grain size was determined

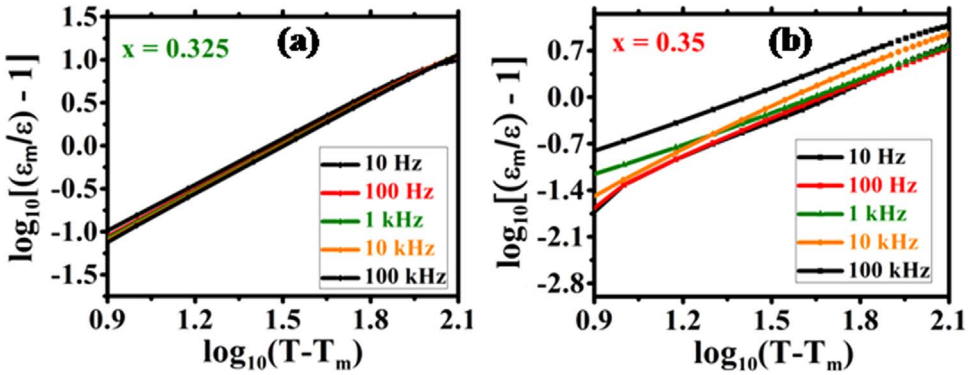

Fig. 9. Variation of $\log_{10}[(\varepsilon_m/\varepsilon)-1]$ *vs* $\log_{10}(T\text{-}T_m)$ for various frequencies (a) 0.675 PMN-0.325 PT and b) 0.65 PMN-0.35 PT. Slope of the linear fit gives the value of relaxor factor γ which is shown in the Table 1. Values of γ attest the relaxor nature of the ceramics samples prepared. Irregular trend in the γ value noticed in the 0.65 PMN-0.35 PT composition may be due to the space charge polarization arise due to the poor adhesion of the silver paste on the ceramic sample.

Table 2
Dielectric analysis of high temperature stabilized samples 0.675PMN-0.325PT and 0.65PMN-0.35PT with frequency in the range 100 Hz to 100 kHz.

Frequency	ε_{max}		$Tan\delta_{max}$		γ	
	32.5	**35**	**32.5**	**35**	**32.5**	**35**
100 Hz	16,470	14,039	0.052	0.063	1.77	1.88
1 kHz	15,703	11,057	0.028	0.062	1.79	1.96
10 kHz	15,295	10,387	0.016	0.023	1.81	1.79
100 kHz	15,033	10,057	0.011	0.028	1.83	1.79

Table 3
Density and piezoelectric coefficient (d_{33}) exhibited by high temperature stabilized samples 0.675PMN-0.325PT and 0.65PMN-0.35PT. Density measurement was carried out using Archimedes' water displacement method and d_{33} was measured on the poled samples.

	0.675PMN-0.325PT	**0.65PMN-0.35PT**
Density	7.719 g/cc (~95.2%)	7.7696 g/cc (~95.9%)
***d*$_{33}$ (3 months after poling)**	390 pC/N	365 pC/N

from the SEM micrograph on the fracture surface of the pellet (Fig. 10). Nearly identical microstructures with bimodal grains pattern, in both the compositions could be the reason for the enhanced electrical response of the samples prepared. Bimodal grains observed are an attestation of the mixed structure in the morphotropic phase boundary [29]. Reduced coercive field observed in the hysteresis loops traced may be attributed to the increased grain growth and reduced grain boundaries in the synthesized ceramics. Presence of bimodal pattern and absence of pyrochlore as observed from the microstructures ensure easy switching of domains, which contributes to the improved electrical response exhibited by the samples.

Table 4
Comparison of ferroelectric and piezoelectric responses exhibited by the compositions studied with identical compositions earlier reported in the literature.

Reference	Composition	P_{sat} (μC/cm^2)	P_r (μC/cm^2)	E_C (kV/cm)	d_{33} (pC/N)
Kumar et al. [36]	x=0.32	29	21	8.7	*325*
This study	**x=0.325**	**23.93**	**19.96**	**5.99**	**390**[a]
This study	**x=0.35**	**32.03**	**25.11**	**6.04**	**365**[a]
Kong et al. [37]	x=0.35	29	19	6.2	–
Algueró et al. [38]	x=0.35	25.6	24	6.2	*137*
Guerra et al. [39]	x=0.35	32	19.1	12	–
Hussain et al. [40]	x=0.36	19.74	13.27	7.55	*490*

[a] Data shown were recorded three months after poling.

4. Conclusions

High temperature stabilization was found to be effective in realizing single phase PMN-PT perovskite, through solid state reaction. We could realize monophasic and device worthy PMN-PT compositions at the MPB (x=0.30, 0.325, 0.35 and 0.375) without using excess PbO in the starting precursors. Absence of non-ferroelectric pyrochlore phase in the synthesized ceramics was established through XRD, Raman spectroscopy, density analysis and microstructure studies. Piezoelectric, dielectric, and ferroelectric properties of the middle compositions x=0.325 and x=0.35

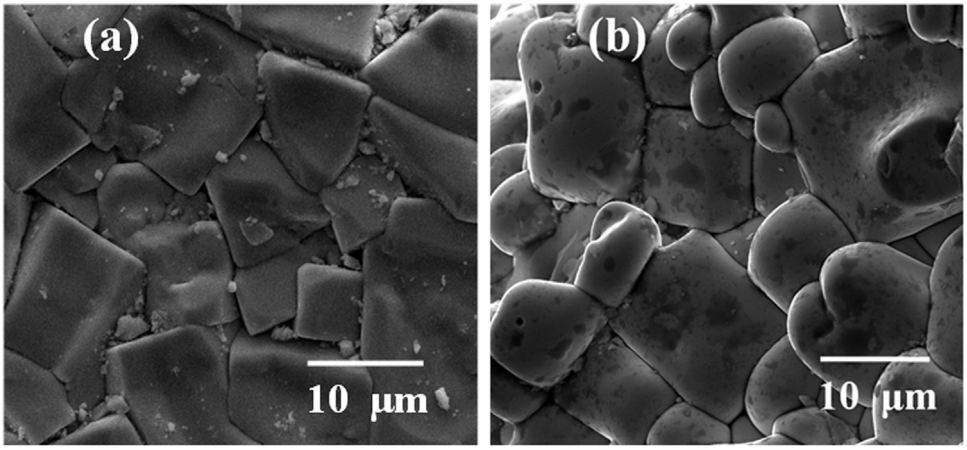

Fig. 10. SEM micrographs of the fractured pellet of samples a) x=0.325 and b) x=0.35 (Machine: Quanta 400 FESEM) (Magnification of 3000× was given for acquiring the images).

were found to be promising. Excellent ferroelectric response x=0.35 composition [P_{sat}=32.03 μC/cm^2, P_r=25.11 μC/cm^2, E_C=6.04 kV/cm, R_{sq}=1.28, Absolute area=3768, range of electric field=−37 to +37 kV/cm and recoverable energy density=59.86 mJ/cm^3], and the outstanding dielectric response of x=0.325 composition [($\varepsilon_{r(max)}$=15,703, Tanδ_{max}=0.02 and γ=1.79 (at 1 kHz)] could be attributed to the structural and micro structural qualities of the ceramics. Excellent piezoelectric response of the ceramics, even at three months after poling (d_{33} −390 pC/N and 365 pC/N for compositions x=0.325 and x=0.35 respectively), ensures the suitability of the method of synthesis as well as the ceramic for device applications. Improved relaxor response of the samples could be established through the analysis of the squareness factor (R_{sq}) of the hysteresis loops traced by the compositions and by studying the relaxor exponents (γ). Energy conversion ability of the ceramics was confirmed by studying the absolute area traced by the hysteresis loops, and recoverable energy calculated for the compositions. The enhanced functional properties of the synthesized single phase perovskite was achieved by the administration of 'stabilization heating' during synthesis and suggests the utility of the method for realization of lead based ceramics.

Acknowledgments

MSR would like to thank (i) Department of Science and Technology (DST), New Delhi, India for providing the funding (SR/NM/NAT/02-2005), that facilitated the establishment of Nano Functional Materials Technology Centre (NFMTC) and (ii) DRDO (Project No: PHY/13-14/286/DRDO/MSRA). A portion of this work has been submitted for granting of Indian patent- No. 2796/CHE/2015 dt. 02/06/2015.

References

[1] M. Tyunina, J. Levoska, A. Sternberg, S. Leppävuori, Dielectric properties of pulsed laser deposited films of $PbMg_{1/3}$ $Nb_{2/3}$ –$PbTiO_3$ and $PbSc_{1/2}$ $Nb_{1/2}$ O 3 –$PbTiO_3$ relaxor ferroelectrics, J. Appl. Phys. 86 (9) (1999) 5179–5184.
[2] D. Viehland, S.J. Jang, L.E. Cross, M. Wuttig, Freezing of the polarization fluctuations in lead magnesium niobate relaxors, J. Appl. Phys. 68 (1990) 2916–2921.
[3] G.H. Haertling, Ferroelectric ceramics: history and technology, J. Am. Ceram. Soc. 82 (4) (1999) 797–818.
[4] O. Bidault, E. Husson, A. Morell, Effects of lead vacancies on the spontaneous relaxor to ferroelectric phase transition in $Pb[(Mg_{1/3}$ $Nb_{2/3})0.9Ti_{0.1}]O_3$, J. Appl. Phys. 82 (1997) 5674–5679.
[5] A.D. Hilton, D.J. Barber, C.A. Randal, T.R. Shrout, On short range ordering in the perovskite lead magnesium niobate, J. Mater. Sci. 25 (1990) 3461–3466.
[6] C. Tantigate, J. Lee, A. Safari, Processing and properties of $Pb(Mg_{1⁄3}Nb)O_3$–$PbTiO_3$ thin films by pulsed laser deposition, Appl. Phys. Lett. 66 (1995) 1610–1613.
[7] M. Tyunina, J. Levoska, Dielectric anomalies in epitaxial films of relaxor ferroelectric $[Pb(Mg_{1⁄3}Nb_{2⁄3})O_3]_{0.68}$-$[PbTiO_3]_{0.32}$, Phys. Rev. B. 63 (2001) (224102-1-224102-8).
[8] A.E. Glazounov, A.K. Tagantsev, A.J. Bell, Evidence for domain-type dynamics in the ergodic phase of the $PbMg_{1/3}Nb_{2/3}O_3$ relaxor ferroelectric, Phys. Rev. B. 53 (17) (1996) 11281–11284.
[9] Z. Feng, T. He, H. Xu, H. Luo, Z. Yin, High electric-field-induced strain of $Pb(Mg_{1/3}Nb_{2/3})O_3$–$PbTiO_3$ crystals in multilayer actuators, Solid State Commun. 130 (2004) 557–562.
[10] R. Cao, G. Li, J. Zeng, S. Zhao, L. Zheng, Q. Yin, The piezoelectric and dielectric properties of $0.3Pb(Ni_{1/3}Nb_{2/3})O_3$–$xPbTiO_3$–$(0.7-x)PbZrO_3$ ferroelectric ceramics near the morphotropic phase boundary, J. Am. Ceram. Soc. 93 (3) (2010) 737–741.
[11] J. Carreaud, P. Gemeiner, J.M. Kiat, B. Dkhil, C. Bogicevic, T. Rojac, B. Malic, Size-driven relaxation and polar states in $PbM_{g1}/3N_{b2}/3_O3$-based system, Phys. Rev. B. 72 (2005) (174115-1-174115-6).
[12] M. Davis, D. Damjanovic, N. Setter, Electric-field-, temperature-, and stress-induced phase transitions in relaxor ferroelectric single crystals, Phys. Rev. Lett. 73 (2006) (014115-1- 014115-16).
[13] A. Slodczyk, P. Daniel, A. Kania, Local phenomena of $(1–x)PbMg_{1⁄3}Nb_{23}O_3$-$xPbTiO_3$ single crystals ($0≤x≤0.38$) studied by Raman scattering, Phys. Rev. B. 77 (2008) (184114-1-184114-16).
[14] D. Vanderbilt, M.H. Cohen, Monoclinic and triclinic phases in higher-order Devonshire theory, Phys. Rev. B. 63 (2001) (094108-1-094108-9).
[15] B. Noheda, D.E. Cox, G. Shirane, S.-E. Park, L.E. Cross, Z. Zhong, Polarization rotation via a monoclinic phase in the piezoelectric $92\%PbZn_{1/3}Nb_{2/3}O_3$–$8\%$ $PbTiO_3$, Phys. Rev. Lett. 86 (17) (2001) 3891–3894.
[16] K.A. Schönau, L.A. Schmitt, M. Knapp, H. Fuess, R.A. Eichel, H. Kungl, Nanodomain structure of $Pb[Zr_{1-x}Ti_x]O_3$ at its morphotropic phase boundary: investigations from local to average structure, Phys. Rev. B 75 (2007) (184117–1-184117-10).
[17] A.K. Singh, D. Pandey, Evidence for *MB* and *MC* phases in the morphotropic phase boundary region of $(1-x)Pb(Mg_{1/3}Nb_{2/3})O_3$ - $xPbTiO_3$: a rietveld study, Phys. Rev. B. 67 (2003) (064102-1-064102-12).
[18] R. Zuo, T. Granzow, D.C. Lupascu, J. Rodel, PMN–PT ceramics prepared by spark plasma sintering, J. Am. Ceram. Soc. 90 (4) (2007) 1101–1106.
[19] Y. Guo, W. Ma, M. Wang, N. Chen, Properties of 0.015PSN–0.3PNN–0.685PZTceramics near morphotropic phase boundary, Mater. Lett. 159 (2015) 126–130.
[20] A. Chauhan, S. Patel, R. Vaish, Multicaloric effect in $Pb(Mn_{1/3}Nb_{2/3})O_3$–$32PbTiO_3$ single crystals, Acta Mater. 89 (2015) 384–395.
[21] S.L. Swartz, T.R. Shrout, Fabrication of perovskite lead magnesium niobate, Mat. Res. Bull. 17 (1982) 1245–1250.
[22] O. Noblanc, P. Gaucher, G. Calvarin, Structural and dielectric studies of $Pb(Mg_{1/3}Nb_{2/3})O_3$–$PbTiO_3$ferroelectric solid solutions around the morphotropic boundary, J. Appl. Phys. 79 (8) (1996) 4291–4297.
[23] P. Augustine, M.S.R. Rao, Realization of device quality PMN–PT ceramics using modulated heating method, Ceram. Int. 41 (2015) 11984–11991.
[24] S.E. Park, T.R. Shrout, Ultrahigh strain and piezoelectric behavior in relaxor based ferroelectric single crystals, J. Appl. Phys. 82 (1997) 1804–1811.
[25] L.P.S. Santos, E. Longo, E.R. Leite, E.R. Camargo, Combined wet-chemical process to synthesize 65PMN-35PT nanosized powders, J. Alloy. Compd. 372 (2004) 111–115.
[26] K.A. Bui-Thi, P. Lecoeur, M. Pham-Thi, G. Garry, Phase optimisation of PMN-PT thin films deposited by Pulsed Laser Deposition on MgO substrates and Pt-coated silicon, IEEE Int. Symp. Appl. Ferroelectr. (2010) 1–4.
[27] M. Shen, G.G. Siu, Z.K. Xu, W. Cao, Raman spectroscopy study of ferroelectric modes in [001]-oriented $0.67Pb(Mg_{1⁄3}Nb_{2⁄3})O_3$– $0.33PbTiO_3$ single crystals, Appl. Phys. Lett. 86 (2005) (252903-1-252903-3).
[28] S. Patel, A.A.B. Moghal, N.A. Madhar, A. Chauhan, R. Vaish, Cyclic piezoelectric energy harvesting in PMN-PT single crystals, Ferroelectr 481 (2015) 138–145.
[29] J.C. Ho, K.S. Liu, I.N. Lin, Study of ferroelectricity in the PMN-PT system near the morphotropic phase boundary, J. Mater. Sci. 28 (1993) 4497–4502.
[30] P. Ravindranathan, S. Komarneni, A.S. Bhalla, R. Roy, Synthesis and dielectric properties of solution sol-gel-derived $0.9Pb(Mg1_{⁄3N}b2_{⁄3})O3.0.1PbTiO3$ Ceramics, J. Am. Ceram. Soc. 74 (12) (1991) 2996–2999.
[31] M. Promsawat, A. Watcharapasorn, Z.G. Ye, S. Jiansirisomboon, Enhanced Dielectric and Ferroelectric Properties of $Pb(Mg_{1/3}Nb_{2/3})_{0.65}Ti_{0.35}O_3$Ceramics by ZnO Modification, J. Am. Ceram. Soc. (2014) 1–7.
[32] S. Ke, H. Fan, H. Huang, H.L.W. Chan, Lorentz-type relationship of the temperature dependent dielectric permittivity in ferroelectrics with diffuse phase transition, Appl. Phys. Lett. 93 (2008) (112906-4-112906-7).
[33] Z. Xia, L. Wang, W. Yan, Q. Li, Y. Zhang, Comparative investigation of structure and dielectric properties of Pb $(Mg_{1/3}$ $Nb_{2/3})O_3$–$PbTiO_3$ (65/35) and 10% $PbZrO_3$-doped Pb $(Mg_{1/3}Nb_{2/3})O_3$–$PbTiO_3$ (65/35) ceramics prepared by a modified precursor method, Mat. Res. Bull. 42 (2007) 1715–1722.
[34] W.S. Hackenberger, J. Luo, X. Jiang, K.A. Snook, P.W. Rehrig, S.Z. Hang, T.R. Shrout, Recent developments and applications of piezoelectric crystals, in: Zuo, G. Ye (Eds.), , Handbook of Dielectric,piezoelectric and Ferroelectric Materials-synthesis, Properties and Applications 3, Woodhead publishing limited, Cambridge, England Ch, 2008, pp. 73–100.
[35] J.A. Horn, S.C. Zhang, U. Selvaraj, G.L. Messing, S.T. McKinstry, Templated grain growth of textured bismuth titanate, J. Am. Ceram. Soc. 82 (4) (1999) 921–926.
[36] P. Kumar, S. Sharma, O.P. Thakur, C. Prakash, T.C. Goel, Dielectric, piezoelectric and pyroelectric properties of PMN–PT (68: 32) system, Ceram. Int. 30 (4) (2004) 585–589.
[37] L.B. Kong, J. Ma, W. Zhu, O.K. Tan, Preparation of PMN–PT ceramics via a high-energy ball milling process, J. Alloy. Compd. 236 (2002) 242–246.
[38] M. Algueró, J. Ricote, R. Jiménez, P. Ramos, J. Carreaud, B. Dkhil, J.M. Kiat, J. Holc, M. Kosec, Size effect in morphotropic phase boundary $Pb(Mg_{1⁄3}Nb_{2⁄3})O_3$–$PbTiO_3$, Appl. Phys. Lett. 91 (11) (2007) 1–3.
[39] J.D.S. Guerra, E.B. Araújo, C.A. Guarany, R.N. Reis, E.C. Lima, Features of dielectric response in PMN–PT ferroelectric ceramics, J. Phys. D*:* Appl. Phys. 41 (22) (2008) 1–5.
[40] A. Hussain, N. Sinha, S. Bhandari, H. Yadav, B. Kumar, Synthesis of $0.64Pb$ $(Mg_{1/3}$ $Nb_{2/3})O$–0.36 $PbTiO_3$ ceramic near morphotropic phase boundary for high performance piezoelectric, ferroelectric and pyroelectric applications, J. Asian Ceram. Soc. 4 (3) (2016) 337–343.